

# Simulation Study on the Effects of Ball Mill and Hydrocyclone Parameters to the P80 of a Pilot-Scale Mineral Processing Plant

**Franco Danilo C. Luistro<sup>1</sup> and Djoan Kate T. Tungpalan<sup>2</sup>**  
*Department of Mining, Metallurgical and Materials Engineering,  
University of the Philippines Diliman, Quezon City 1101, Philippines  
Corresponding author: fcluistro1@up.edu.ph<sup>1</sup>*

**Abstract** – Comminution is considered as one of the most energy intensive operations in metal recovery. It is here that the target particle size, P80, is achieved to facilitate mineral liberation for the effective recovery of the valuable minerals. To facilitate a high degree of liberation, ore particle sizes should be within the range of the valuable mineral particle sizes. Simulations have proven effective in helping optimize mineral processing operations and increase efficiency. However, simulation studies that cover small- to pilot-scale mineral processing operations are still quite limited. In this study, the grinding circuit of a pilot-scale mineral processing plant located in Itogon, Benguet was used as basis for MDK simulations to study the effects of ball mill and hydrocyclone parameters to the P80 in processing gold ore consisting primarily of calcite, quartz, and considerable amounts of sulfides. The study has indicated that a lower ball mill critical speed fraction, and a smaller vortex finder diameter decreases the overall comminution product particle size while the operating % solids inside the ball mill and the hydrocyclone spigot diameter has the opposite effect. A lower cyclone overflow % solids also indicate finer P80.

**Keywords:** Mineral Processing, Simulations, Ball mill, hydrocyclone

## I. INTRODUCTION

High demand for different metals to bolster industrialization and development has greatly accelerated the mining industry. Previous deposits that were deemed to be non-viable for extraction are now being considered as potential sources of raw materials. Thus, the need for more cost-effective measures in determining the possible processing outcomes arise as exploration and development of these new mining and mineral processing plants increase in difficulty due to factors like mineralogical complexity, lower metal grades, higher consumable costs, among others [1][2].

The introduction of simulations-based analysis on estimating recoveries based on mineralogical data has proven to be an important tool in assessing the feasibility of current and future mining projects. This has greatly reduced the risks involved in mineral exploration and mining while also bridging different aspects involved in the mine production [3].

From these simulation studies, there are only a handful that tackle the small-scale mining industry. Most of them focused only on minimizing or mitigating the hazards caused by the

small-scale mining activities to the environment and human health. Little research has been made or published with regards to optimizing the small-scale operations. Moreover, improving the small-scale mining operations with the aid of modern technologies, such as modelling and simulations, has not been performed.

The study aims to determine the effects of varying parameters like the ball mill critical speed ratio, ball mill operating % solids, cyclone overflow % solids, cyclone spigot diameter and cyclone vortex finder diameter on the particle size distribution of the grinding products of a pilot-scale mineral processing plant. This study utilized ore obtained in Itogon, Benguet, specifically in the "Pink Tunnel" located in Brgy. Gumatdang and the simulations were done using the Model Development Kit or MDK software.

The MDK is a software framework designed to perform mineral processing circuit simulations using multi-component models programmed by Michal Andrusiewicz from the University of Queensland, Australia in 2017 [4]. This software was developed as part of the doctoral thesis dissertation entitled, "*Modelling and Simulation Approaches for Exploiting Multi-Component Characteristics of Ores in Mineral Processing Circuits*", by Bianca Foggiatto from the same university.

Simulations done by this software allow the user to construct their mineral processing flowsheets by linking the corresponding single and multi-component models to the same interface. A simple diagram on the corresponding input-output of the MDK simulation model is shown in Figure 1.

The system runs simulations one process at a time with the order based on the input flowsheet. The resulting stream characteristics from the first component model is fed to the succeeding component model. The next component of the system then only takes the necessary data for the simulations to be done.

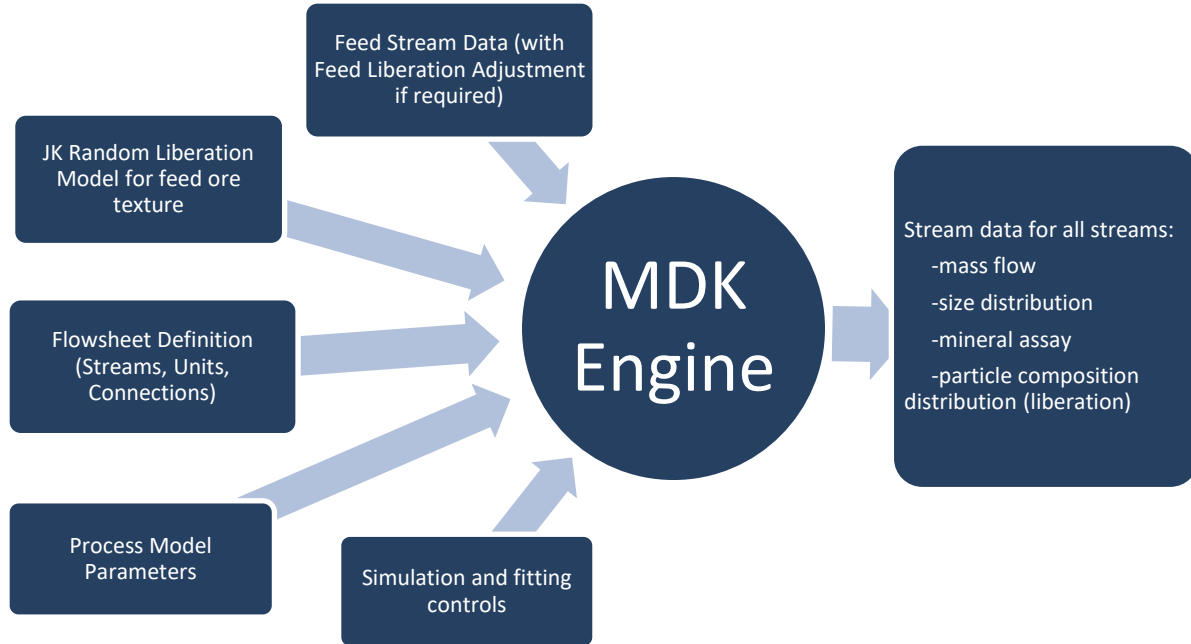


**Figure 1.** MDK Simulation model. [4]

The MDK engine considers several process stream characteristics such as the material’s particle size distribution and the corresponding mineral composition. Ore and mineral characteristics like specific gravity and work index can also be taken into consideration. The system uses MS Excel worksheets as the interface, with the core of the MDK simulations making use of Visual Basic to call out the codes that are based on JKSimMet models and programmed using Fortran.

## II. METHODOLOGY

The general work flowsheet conducted in this research can be seen in Figure 2.

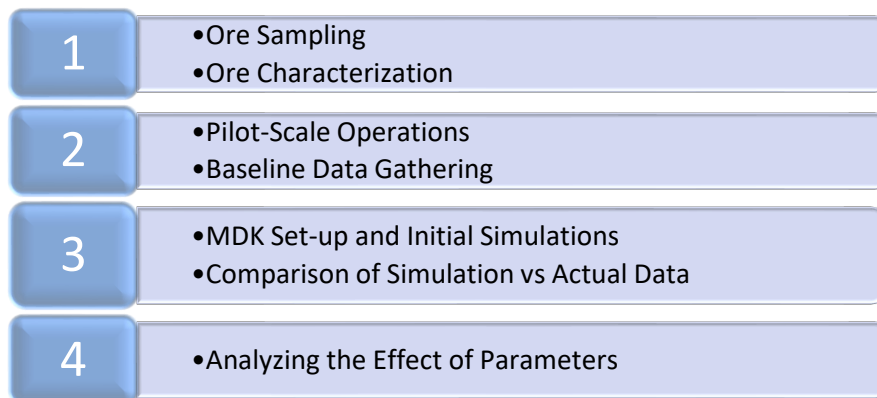


**Figure 2.** Experiment Methodology flowsheet

The ore used for the study came from the “Pink Tunnel”, a small-scale mining tunnel located in Brgy. Gumatdang, Itogon, Benguet. Representative samples were taken by using the coning and quartering technique to obtain the required sample sizes for succeeding tests.

From the representative sample, around 1000 grams of dried ore with mesh-of-grind of 75 microns was taken and subjected for a modified version of the Bruce Method for gold occurrence to determine the total gold content and deportment. This method is a series of leaching processes using different lixivants to dissolve the gold content of the ore associated with different mineral species in the ore.

Another set of samples was also taken to undergo mineralogical analysis to verify and determine the ore’s mineral content. This was done by taking petrographs from thin and polished sections of the samples and analyzing the ore samples using X-ray Diffraction for mineral identification and estimation.

Pilot-scale comminution was also done using a circuit composed of a primary jaw crusher and a secondary roll crusher as the crushing stage. The products are directed to a fine ore bin before being fed to a ball mill – hydrocyclone circuit for grinding. The flowsheet of the comminution circuit being studied is shown in Figure 3.

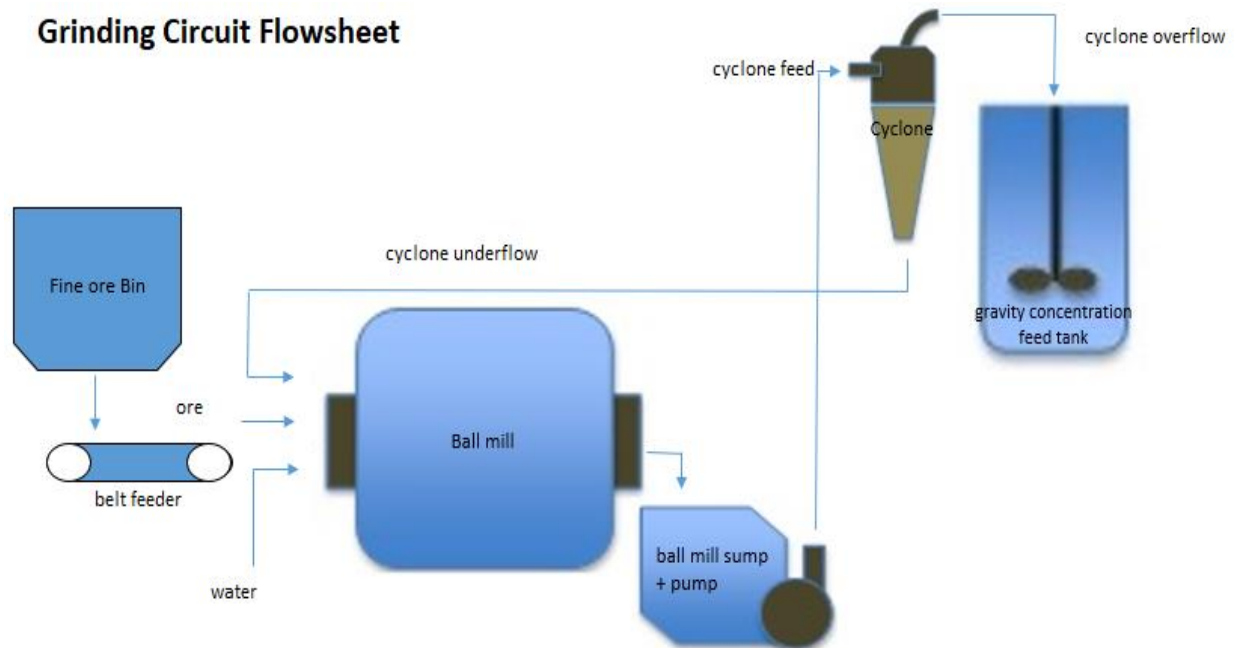


**Figure 3.** Grinding circuit flowsheet used by the pilot-scale plant.

The initial settings and operating parameters used for the equipment involved during the grinding section of the comminution circuit were recorded while the plant was being operated.

In addition to monitoring the parameters while the plant is operating, samples were also collected at 15-minute intervals from the fresh ore feed, hydrocyclone overflow, and hydrocyclone underflow for particle size analysis.

Results from the mineralogical analysis of the fresh ore feed, and the dimensions and operating parameters of the grinding equipment were used for setting-up the model development kit used (MDK) used for the simulations. This involves the initial feed particle size analysis, the mineralogy of the ore, the actual equipment sizes used in the plant, along with the operating parameters used while running it.

Once the MDK has been set up, an initial test was done, and the results were compared with the actual pilot-scale runs to determine if the MDK simulator will produce results that can be used as basis for studying the effects of parameters and in predicting the desired P80 of the ore. Three (3) actual pilot plant runs were conducted and were used for verification. A total of 5 metric tons of ore coming from the same bulk where mineralogical samples were taken were used for each of the pilot-scale runs.

Once the simulation results were confirmed close to the actual pilot-scale runs, the values of the parameters to be studied were varied and simulation runs were done to obtain the corresponding effects on grinding performance. A one-factor-at-a-time approach was done in analyzing the data obtained from MDK simulations for the individual effects of each parameter studied. This is based on the nature of parameter adjustments, especially in manual circuits, normally being implemented in processing plants where only one parameter is being adjusted to achieve the target P80 from the grinding circuit.

These parameters were chosen as they were determined to play an important role in determining the effectiveness of milling [5]. They also proved to be the easiest parameter to adjust and modify if necessary. These parameters are ball mill critical speed fraction, ball mill operating % solids, hydrocyclone overflow % solids, hydrocyclone spigot diameter, and hydrocyclone vortex finder. Five levels for each factor being studied were done to be able to establish a trend with the grinding performance, particularly the P80.

It should be noted that for a better classification in the hydrocyclone, the ball mill discharge is usually diluted with water before entering the hydrocyclone. However, due to the difficulty of measuring the slurry density of the hydrocyclone feed in actual operations, it was decided to correlate the P80 with the resulting hydrocyclone overflow % solids in identifying the effect of the hydrocyclone feed dilution since the actual pilot-scale runs showed that hydrocyclone feed % solids are correlated with the hydrocyclone overflow % solids.

### **III. RESULTS AND DISCUSSION**

Results from the Bruce method analysis for gold department shows that the total gold content of the ore is 5.3861 grams per ton of ore. The data also indicates that the bulk of the gold in the ore, comprising 71.72% (3.86 gpt Au) of the total gold, can be found within the sulfide matrix, while a considerable amount (19.96% or 1.07 gpt Au) also exists as free or

exposed particles. Gold that is locked in carbonates consists of only a small portion at 7.29% (0.39 gpt Au) of the total available gold and approximately 1.01% (0.05 gpt Au) is deemed to be unrecoverable and trapped within the insoluble gangue minerals.

The images from the thin sections show that the samples contained minerals such as calcite, quartz, and other opaque materials that were perceived to be sulfides. A sample image taken from the sample thin section can be found in Figure 4. The ore was found to be composed primarily of calcite and quartz that make up approximately 53.00% and 41.67% respectively. Opaque materials were also estimated to be at around 5.33% of the ore component.

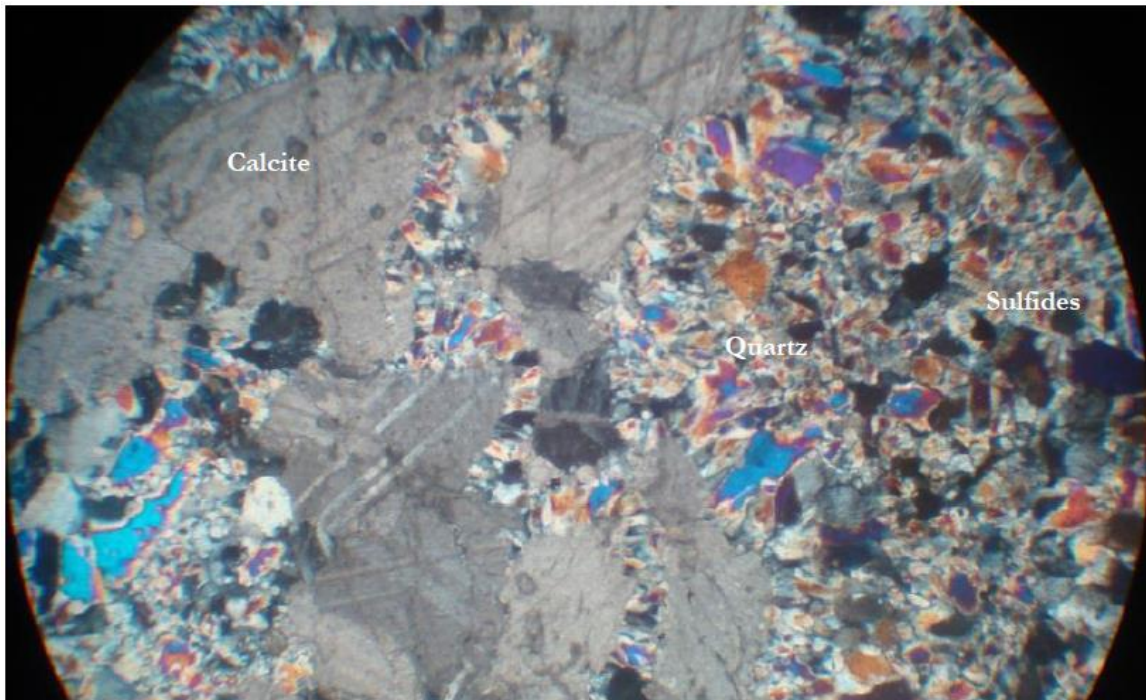


**Figure 4.** Thin section showing deposition of quartz and replacement of calcite. Opaque minerals mostly consist of sulfides that are hosted in quartz. FOV length of 4.22mm

Upon further analysis, using the polished sections of the samples shown in Figure 5, it was confirmed that pyrite (py), chalcopyrite (cpy) and some amount of galena (gal) compose the majority of the opaque materials. Small inclusions of galena can also be seen in Figure 5B along with a small speck of gold attached to the chalcopyrite particle.

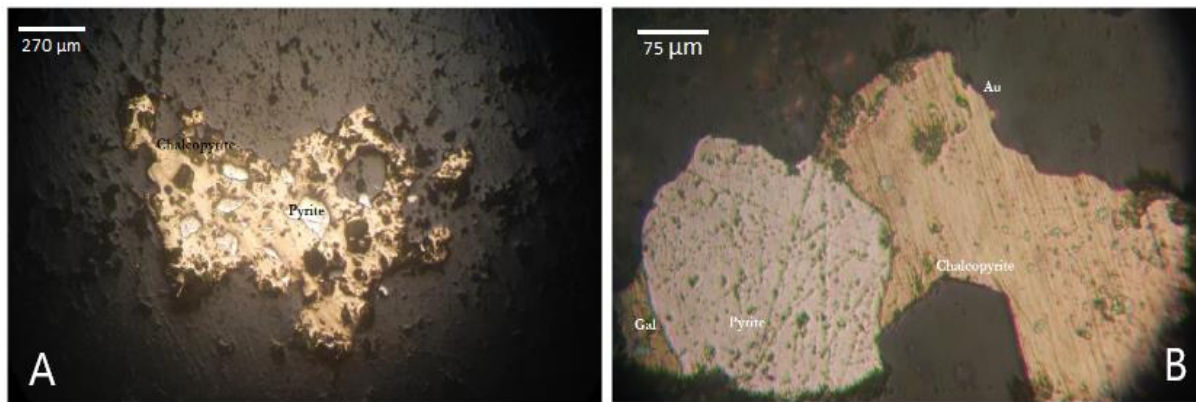


**Figure 5.** [A] Chalcopyrite seen as an intergrowth with pyrite; [B] The same specimen showing a gold particle attached to the chalcopyrite grain.

X-ray diffraction analysis of the samples using CuK $\alpha$  wavelength of 1.54Å, reported by the National Institute of Geological Sciences also confirm the presence of quartz (qtz), sphalerite (sp), galena (gal), pyrite (py), chalcopyrite (cpy), calcite (cc), rhodochrosite (rhod), illite (mi), and epidote (ep). Figure 6 shows the XRD result with the corresponding peaks of the said minerals labeled accordingly.

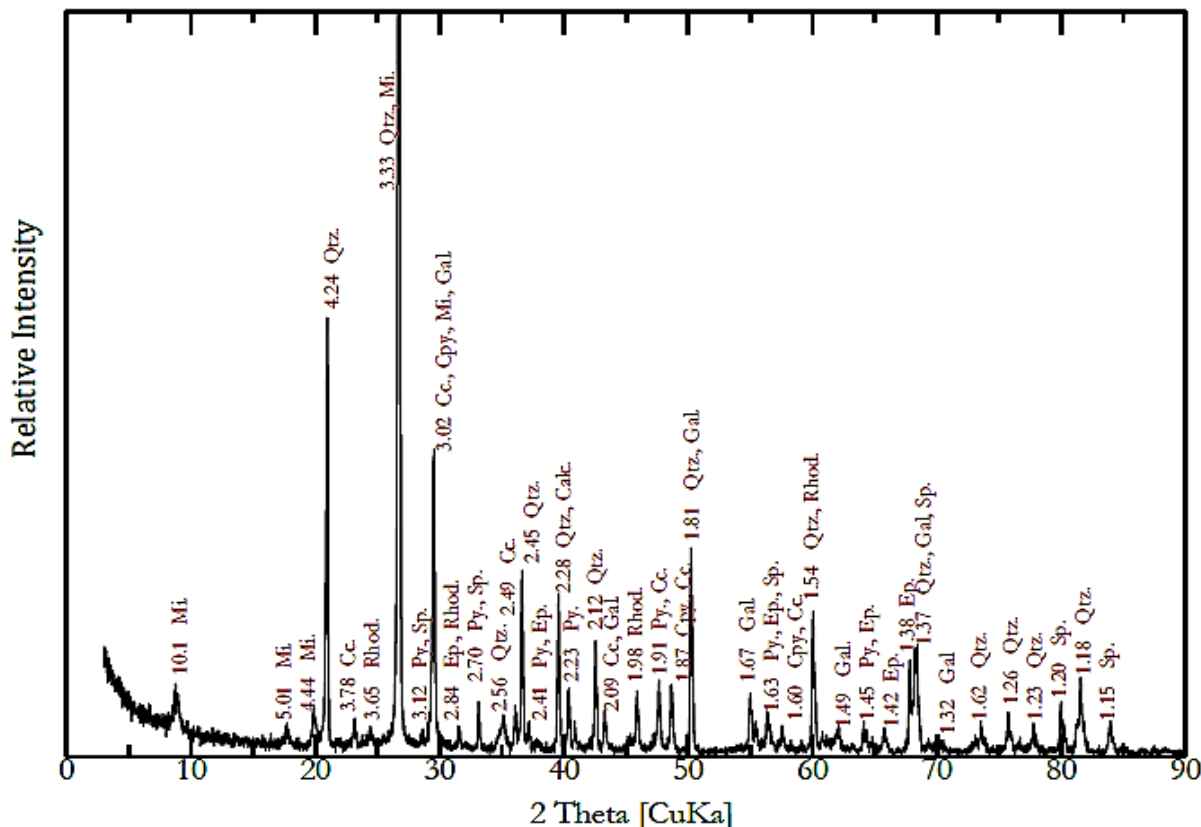


**Figure 6.** XRD result for the samples submitted to the National Institute of Geological Sciences.



The equipment specifications and baseline parameters used during operations were recorded and indicated in Tables 1 and 2. The ball mill and hydrocyclone specifications were obtained from their manufacturer while the operating parameters were process targets made during operations.

**Table 1.** Ball mill dimensions and parameters maintained during operations.

<b>Ball Mill Dimension and Parameters</b>	
Size	3 ft. diameter x 6 ft. length
Critical Speed	34.5 rpm
Mill Speed	28 rpm, 81.16% critical speed
Ball Load	2 tons, 30% volume
Ball Size	2 inches
Trunnion diameter	6 inches
feed rate	1.50 tph
BM discharge % solids	70-72%

**Table 2.** Hydrocyclone dimensions and parameters maintained during operations.

<b>Hydrocyclone Dimension and Parameters</b>	
hydrocyclone diameter	4 inches
vortex finder	1 inch (0.025m)
apex/spigot	3/8 inch (0.010m)
inlet diameter	1.5 inches
length of cylinder	6 inches
operating pressure	50 psi
hydrocyclone feed % solids	58-60%
hydrocyclone overflow % solids	36-40%
hydrocyclone underflow % solids	72%

Data from ore characterization like initial particle size distribution, mineral composition and densities, equipment specification and operating parameters were used as input for running the simulations in MDK. An initial assumption is that the mineral composition across all particle sizes is the same and that all the system components behave as expected from existing mineral processing models as the MDK is limited to these models at the time of development.

The resulting product particle size distribution and 80% passing are then compared with the obtained result from the actual mineral processing plant runs which can be seen in Figure 7.

The data from the three pilot-scale runs presented similar particle size distributions. It should be noted that the simulation presents a relatively higher number of fine particles compared to the actual plant runs.



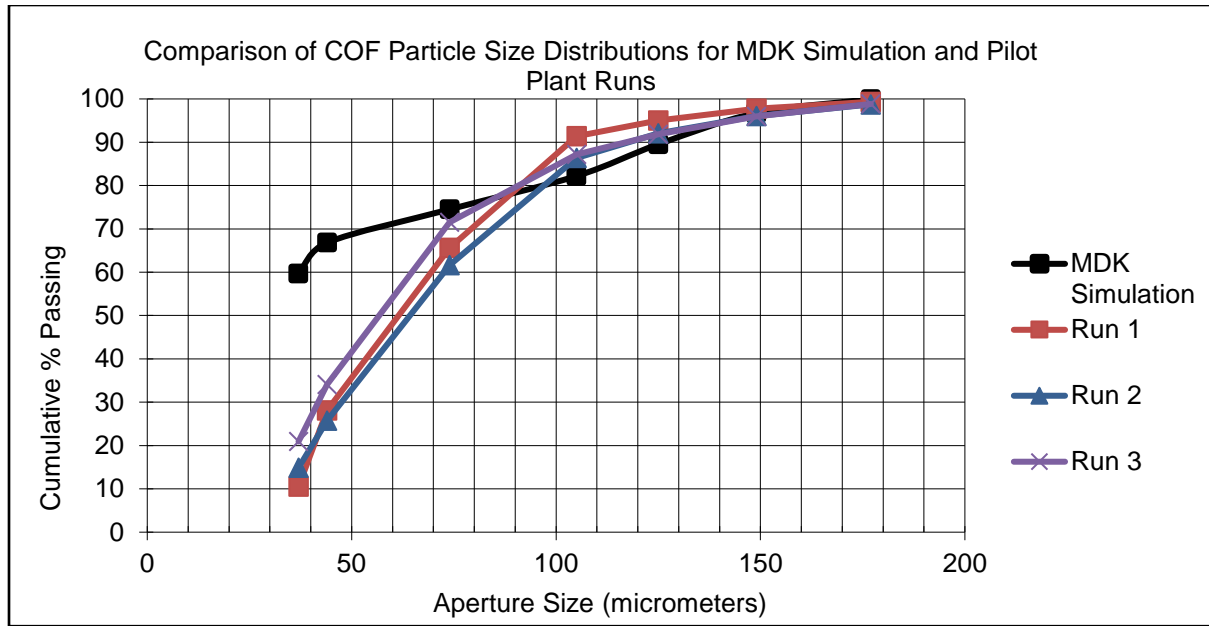


**Figure 7.** Comparison of cyclone overflow particle size distributions of pilot plant runs and MDK simulation.

The difference in the distributions between the actual plant runs can be explained by the agglomeration of fine particles to the coarse fraction resulting to a lower number of fine particles when weighed per size fraction. Aside from this, the input and output for the simulation accounts for the absolute particle size distribution of the ore and does not consider ore texture and particle to particle agglomeration [6].

Given that the particle size analysis on all the pilot plant runs produced near-identical particle size distributions, the resulting 80% passing from the distributions also presented values that are close to each other. The average P80 of the three pilot-scale runs was calculated at 92.67 microns. The result from the MDK simulation on the other hand indicates a product particle size with 80% passing 95 microns.

A t-test was conducted to determine if the mean of the pilot-scale runs (92.67 microns, SD = 3.79 microns) was statistically different from the mean of the MDK simulation results ( $\mu_0$ ). At a 95% confidence level, the null hypothesis that the two means are equal was not rejected. This suggests that the MDK simulation results can be considered a valid basis for modeling pilot-scale runs.

The trend obtained from the simulations indicates that for ball mill critical speed fractions between 75.2% to 87.2%, a linear relationship between the grinding product size and ball mill critical speed fraction can be observed. Figure 8 shows that decreasing the operating speed of the ball mill also decreases the product particle size.

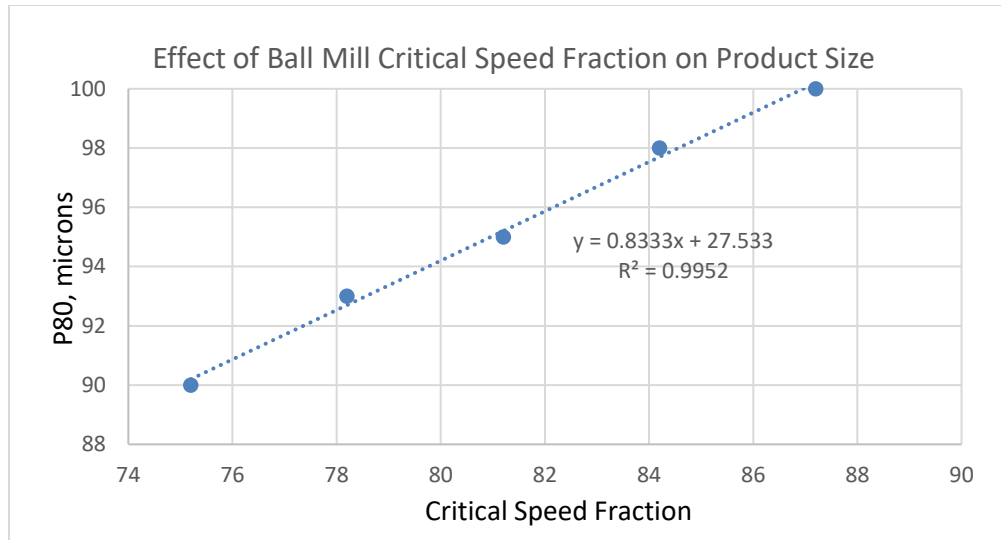


**Figure 8.** Effect of Ball mill Critical Speed fraction on the P80 of the grinding products.

The decrease in the grinding product size can be highly attributed to the increased breakage rate for finer size fractions at lower speeds observed in tumbling mills [7]. Lower mills speed increases cascading motion of the charge inside the mill resulting to abrasion. As a mode of particle size reduction, abrasion produces more fine particles that are chipped-off of the larger particles that rub-off and collide against each other and the grinding media while inside the ball mill [8,9].

Simulation results also showed that grinding product particle size decreases as the percent solids in the slurry inside the ball mill is increased. The trend was observed for the range of slurry densities between 66% to 78% solids slurry inside the ball mill. Figure 9 shows the relationship between the % solids of the slurry inside the ball mill versus the resulting grinding product particle size.

When the % solids in the slurry increases, the viscosity of the slurry is also increased. Changes in the slurry viscosity greatly affect the slurry's rheological properties which can be considered as a key parameter that influences the mixing of the charge inside the tumbling mill [10]. The majority of the motion of the charge inside the mill, and hence the particle size reduction, occurs near the surface of the media bed where cascading motion is more dominant. Cascading motion results in abrasion which produces finer particles. Similarly, a higher slurry density provides higher chances for particle-to-particle breakage [8,9]. The ore particles act as grinding media by chipping the particle surface producing finer particles.

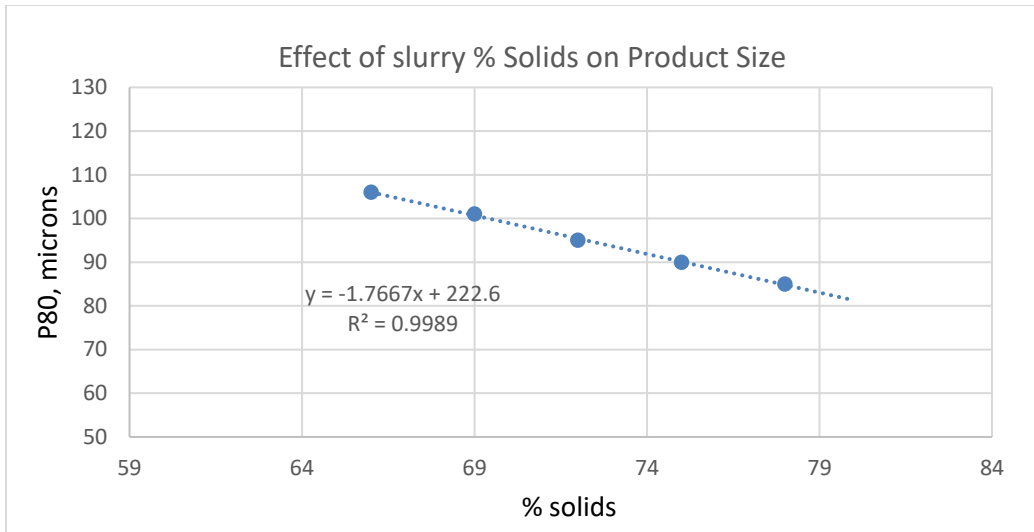


**Figure 9.** Effect of Slurry % solids inside the Ball Mill on the P80 of grinding products.

Observations on the variables of ball mill operations also showed that by lowering slurry % solids, the probability of grinding media-to-ore particle collision may decrease. This in effect decreases the effective particle size reduction of ore happening inside the mill [11]. However, it was also observed that operating at a lower solids density inside the mill can be damaging to the mill liners [11].

Further evaluating the parameters, the slurry density of the cyclone feed is the main parameter usually controlled to provide a better classification of particles as they exit the cyclone. However, due to the difficulty in determining the cyclone feed slurry density in actual pilot-scale operations, the cyclone overflow % solids were used as reference for varying the slurry density of the cyclone feed instead. With the application of slurry controls on the cyclone feed, it was found that the grinding product particle size can be associated with the % solids of the slurry as it comes out of the cyclone as can be seen in Figure 10.

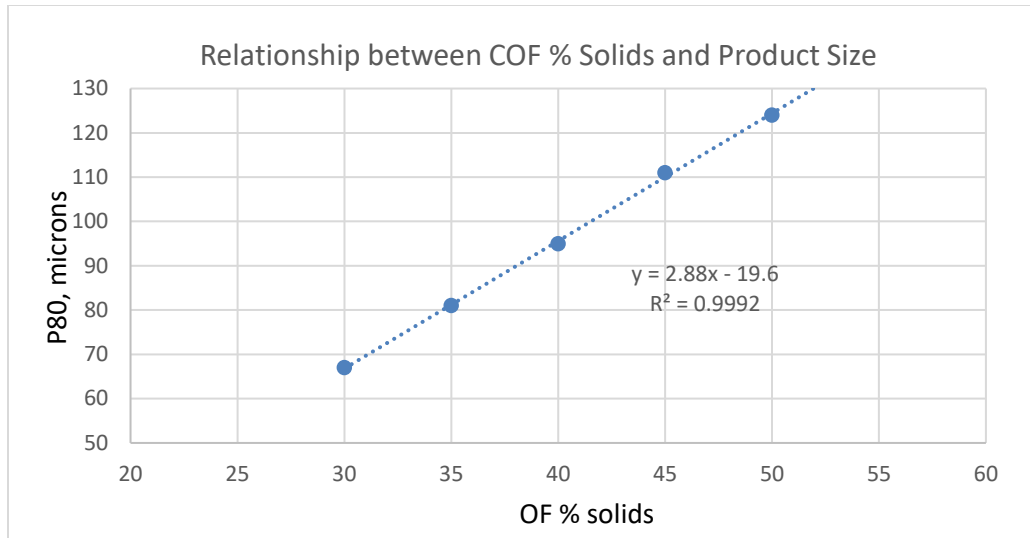


**Figure 10.** Relationship between the hydrocyclone overflow % solids and the P80 of the grinding products.

The results indicate that the % solids of the cyclone overflow slurry can be associated with the P80 of the comminution products for the range between 30% to 50% solids studied. Higher cyclone overflow % solids indicate coarser P80 values of the grinding products.

Decreasing the number of solids in the feed slurry is found to be an effective way of improving particle classification in the hydrocyclone [12]. Lower solids density makes it easier for particles to segregate as they move along the slurry path inside the hydrocyclone.

By increasing the diameter of the hydrocyclone spigot, simulation results show that a corresponding decrease in the measured P80 of the comminution products can be observed as shown in Figure 11.

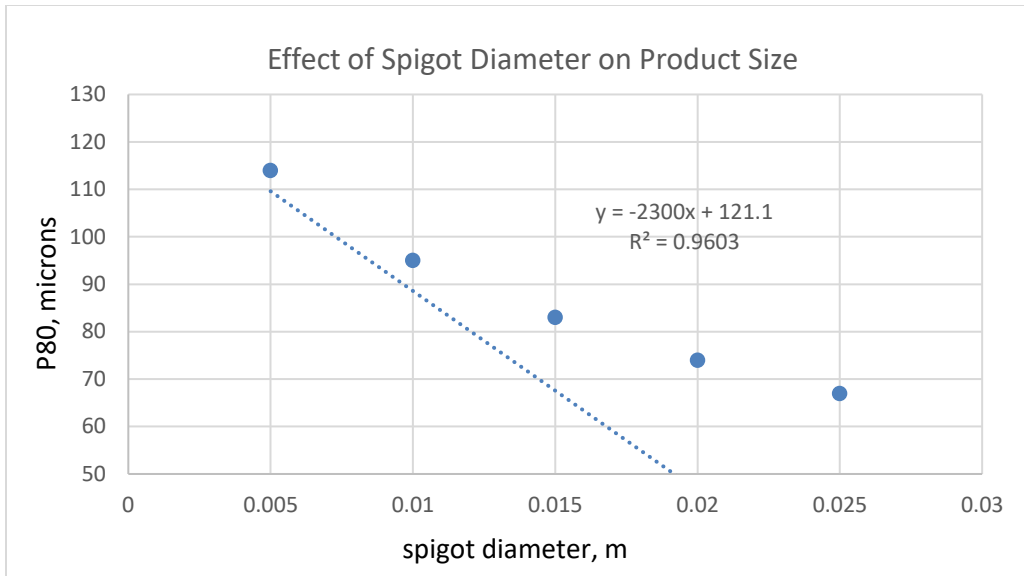


**Figure 11.** Effect of hydrocyclone spigot diameter on the P80 of the grinding products.

The diameter of the cyclone spigot generally affects the residence time of the slurry inside the cyclone. A larger spigot diameter allows the faster discharge of the underflow that would include more fine particles. Smaller spigot diameters, in contrast, would force the heavy and coarse materials to the secondary vortex, then out to the cyclone overflow [13]. It should be noted that the observed relationship may only be valid within the range of 0.005m – 0.025m spigot diameter as evaluated in this study.

Lastly, for the range of vortex finder diameter in this study (0.015m – 0.035m), we can see a general increase in the P80 of the grinding products while increasing the vortex finder diameter, as illustrated in Figure 12.

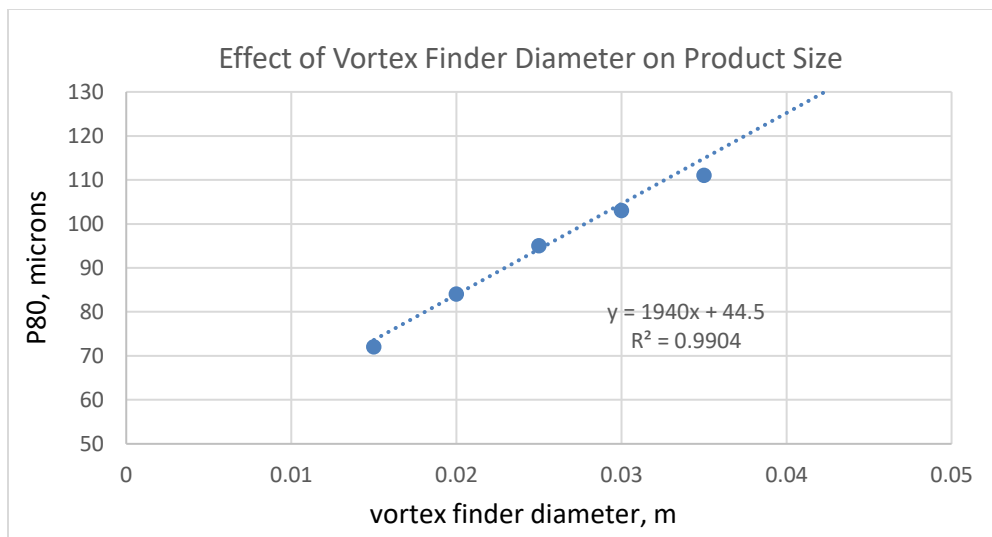


**Figure 12.** Effect of vortex finder diameter on the P80 of the grinding products.

During operation of a hydrocyclone, particle size segregation patterns indicate that coarser particles are generally being pushed outward along the cyclone wall while the finer particles can be found in the interior part of the cyclone [14]. This creates an increasing average particle size profile as you go from the center of the hydrocyclone outward, to the hydrocyclone wall.

Since the vortex finder acts as the collection point or exit for the overflow, changes in the diameter of the vortex finder would affect the overall particle size distribution of the slurry coming out of the cyclone. As the vortex finder diameter changes, the portion of the secondary vortex that can exit through the vortex finder also changes. When decreasing the diameter of the vortex finder, only the finer particles located close to the middle of the cyclone, in the secondary vortex, will be collected. Whereas a wider range of particle sizes can be accommodated when the vortex finder diameter is increased.

#### IV. CONCLUSIONS AND RECOMMENDATIONS

In the simulations done by varying one factor at a time, it was found that the general trend for the P80 of the grinding product increases as the ball mill critical speed fraction, cyclone overflow % solids, and cyclone vortex finder diameter are increased. On the other hand, the P80 decreases when the target % solids inside the ball mill, and the cyclone spigot diameter are increased.

The simulation and the actual pilot plant runs resulted in comparable P80. The average P80 of the actual pilot plant runs is 93 microns while the MDK simulation resulted in a P80 of 95 microns.

Based on the results and analysis obtained from MDK simulations, the following can be recommended: First, conducting tests for other types of ore to further support the use of simulations for smaller scale mineral processing operations; Second, additional studies to determine the effects of other parameters like the ball mill loading, grinding media size, hydrocyclone diameter, etc. can also be explored.

#### References:

- [1] Mudd G, Jowitt S. 2016. From mineral resources to sustainable mining – The key trends to unlock the Holy Grail? The Third AusIMM International Geometallurgy Conference; Perth, WA, Australia. p. 37-54.
- [2] Powell M. 2013. Utilising orebody knowledge to improve comminution circuit design and energy utilization. The Second AusIMM International Geometallurgy Conference; Brisbane, QLD, Australia. p. 27-35.
- [3] Lishchuk V, Koch P, Ghorbani Y, Butcher A. 2020. Towards integrated geometallurgical approach: Critical review of current practices and current trends. *Minerals Engineering*. 145:106072.
- [4] Andrusiewicz M, Brennan M, Evans C, Morrison R, Perkins T, Wightman E. 2011. Multi-component modelling and simulation, AMIRA International P90 Final Technical Report. p. 119-204.
- [5] Rizlan Z, Mamat O. 2014. Process parameter optimization of silica sand nanoparticles production using low speed ball milling method. *Chinese Journal of Engineering*. 2014:802459.
- [6] Parapari PS. 2020. Effect of loading mechanism and ore texture on ore breakage – A multi-dimensional study. Lulea University of Technology, Graphic Production.

- [7] Napier-Munn T, Morrell S, Morrison R, Kojovic T. 1996. Mineral comminution circuits: Their operation and optimization. Julius Kruttschnitt Mineral Research Center. University of Queensland; Indooroopilly, QLD, Australia.
- [8] Gupta A, Yan DS. 2016. Mineral processing design and operation: An introduction. 2<sup>nd</sup> ed. Elsevier Science. p. 421-469.
- [9] Wills B, Napier-Munn TJ. 2005. Wills' mineral processing technology. An Introduction to the Practical Aspects of Ore Treatment and Mineral Recovery. 7<sup>th</sup> ed.
- [10] Haas B, Bosch A, Kottgen A, 2012. Effect of slurry density on load dynamic and milling performance in an iron ore ball mill – On-line estimation of in-mill slurry density. Comminution Conference; Cape Town, South Africa.
- [11] Paul O. Abbe@. 1999. Retrieved from <https://www.pauloabbe.com/size-reduction/resources/variables-in-ball-mill-operation> on 5 Sept 2024.
- [12] Weir. 2020. Retrieved from <https://www.global.weir/newsroom/global-news/how-to-resolve-the-most-common-hydrocyclone-problems/> on 5 Sept 2024.
- [13] Multotec. 2017. Retrieved from: <https://www.multotec.com/en/news-articles/cyclones-three-ways-to-maintain-high-performance> on 5 Sept 2024)
- [14] Narasimha M, Brennan M, Holtham P. 2012. CFD modelling of hydrocyclones: Prediction of particle size segregation. Minerals Engineering. 39:173-183.